Friction **5**(2): 155–170 (2017)
DOI 10.1007/s40544-017-0141-2
ISSN 2223-7690
CN 10-1237/TH
RESEARCH ARTICLE

Surface roughness measurements in NFMQL assisted turning of titanium alloys: An optimization approach

Munish K. GUPTA*, P. K. SOOD
MED, NIT, Hamirpur (H.P.) 177005, India
Received: 19 September 2016 / Revised: 26 October 2016 / Accepted: 11 December 2016

Abstract: The prediction and optimization of surface roughness values remain a critical concern in nano-fluids based minimum quantity lubrication (NFMQL) turning of titanium (grade-2) alloys. Here, we discuss an application of response surface methodology with Box–Cox transformation to determine the optimal cutting parameters for three surface roughness values, i.e., R_a, R_q, and R_z, in turning of titanium alloy under the NFMQL condition. The surface roughness prediction model has been established based on the selected input parameters such as cutting speed, feed rate, approach angle, and different nano-fluids used. Then the multiple regression technique is used to find the relationship between the given responses and input parameter. Further, the experimental data were optimized through the desirability function approach. The findings from the current investigation showed that feed rate is the most effective parameter followed by cutting speed, different nano-fluids, and approach angle on R_a and R_q values, whereas cutting speed is more effective in the case of R_z under NFMQL conditions. Moreover, the predicted results are comparatively near to the experimental values and hence, the established models of RSM using Box-Cox transformation can be used for prediction satisfactorily.

Keywords: nano-fluids; optimization; surface roughness; turning; titanium alloy

1 Introduction

Nowadays, surface finishing is considered as a critical performance parameter in various manufacturing industries that appreciably affects the mechanical properties of parts namely creep life, resistant to corrosion and fatigue behavior. It additionally influences other useful qualities of machined parts like wear, friction, lubrication, heat transmission and electrical conductivity [1]. Thus, accomplishing good surface quality is of immense significance for the usefulness of the machine parts [2]. The various factors such as cutting speed, feed rate, depth of cut, and tool material directly affect the surface quality of the machined parts [3]. Among these factors, the uses of cutting fluids are still considered as one of the major factors [4]. Cutting fluids not only improve the surface finishing by reducing the cutting temperature, but also provide the proper lubrication effect between the tool-chip interfaces. The various sorts of environmentally friendly strategies such as dry machining, minimum quantity lubricant (MQL) and nano-fluids with MQL, have been presently developed to increment the overall efficacy of the machining process [5].

Dry machining is not feasible during machining of difficult to cut and sticky materials like titanium base alloy, because these materials when machined dry tend to stick to the tool face leading to tool failure and result in a poor surface finish on the machined surface [6]. Therefore, the use of the MQL technique can be regarded as an attractive alternative solution, in which a very small amount of cutting fluid along

* Corresponding author: Munish K. GUPTA, E-mail: munishguptanit@gmail.com

NOMENCLATURE

a_p, Depth of cut (mm)
V_c, Cutting speed (m/min)
ANOVA, Analysis of variance
CBN, Cubic boron nitride
MoS_2, Molybdenum disulfide
R_a, Average roughness (μm)
R_z, Maximum peak to valley (μm)
SEM, Scanning electron microscopy
f, Feed rate (mm/rev)
ϕ, Side cutting edge angle or approach angle (degree °)
Al_2O_3, Aluminium oxide
C.F., Cutting fluid
NFMQL, Nano-fluids based minimum quantity lubrication
R_q, Root mean square (μm)
RSM, Response surface methodology

with compressed air is directly applied to the machining area through the set of nozzles by drop-by-drop and mist [7, 8]. The MQL technique with nano-particles (nano-fluids) also contributes to greener or cleaner manufacturing, as the harmful effects of other MWFs are completely eliminated from the machining process [5].

A perusal of current literatures provides numerous studies which primarily focus on nano-fluids with the MQL technique in various machining operations. For the first research group, the grinding experiments were performed by Shen et al., on cast iron to evaluate the tribological behavior and performance of novel MoS_2 nano-particles. The outcome seems that the cutting fluid with novel MoS_2 nano-particles drastically reduce the friction and grinding force [9]. Several other researchers, namely Ramesh et al. [10−12], Sridharan and Malkin [13], Kwon and Drzal [14], Nam et al. [15], Samuel et al. [16], Park et al. [17], Vasu and Reddy [18], Ramesh et al. [19], Khanderkar et al. [20], Kalita et al. [21], Nguyen et al. [22], Amrita et al. [23], Paul and Varadarajan [24], Srikiran et al. [25], Amrita et al. [26], Sharma et al. [27], Su et al. [28] and Gupta et al. [5] have applied different nano fluids in various sorts of machining operations. Table 1 clearly describes that, the use of nano-particles with MQL in machining has proved to be an effective method to minimize the given responses. Moreover, some former researchers such as Barzani et al. [29, 30] and Unune et al. [31] presented the various prediction model used for estimating the surface roughness values (as described in Table 1). From the published works in the scientific database, it has been revealed that, the majority of work done under NFMQL has been carried out on various other materials, such as EN 24 alloy steel, Inconel-600 alloy, Ti-6Al-4V alloy, AISI 4340 steel, AISI 1040 steel, AISI 316L steel etc., and the general machining characteristics in terms of cutting forces, tool wear, cutting temperature and arithmetic average surface roughness (R_a) have been investigated. But, to the best of our knowledge, till now there has not been any systematic study conducted on turning of titanium (grade-2) alloy under NFMQL conditions while considering three surface roughness values, i.e., average roughness (R_a), root mean square (R_q), and maximum peak to valley (R_z). However, this does not exclude its importance, as there are also highly used alloys in orthopedic applications, such as implants and prosthesis, airframe and aircraft engine parts, marine chemical parts, condenser tubing and heat exchangers. Apart from this, it is totally resistant to corrosion. Thus, it would be interesting as well as enlightening to study the machining characteristics of this particular grade such as titanium (grade-2) alloy considering NFMQL conditions. Therefore, this study represents the first attempt to investigate the effect of process parameters while turning titanium (grade-2) alloy under NFMQL conditions by using response surface methodology (RSM) with Box–Cox transformation. For this purpose, the series of experiments on the CNC turning center have been performed. After that, the input (machining parameters) and output (surface roughness values) data have been collected (1) to develop the prediction model by using RSM with Box–Cox transformation, (2) to study the effect of machining parameters on surface roughness values, and (3) to optimize the machining parameters by using the desirability function approach.

Table 1 Literature survey/ work done using the NFMQL technique.

References	Author and year	W/P material	Type of nano-particles used	Machining operation	Investigations/findings
[10]	Ramesh et al., 2008	Ti-6Al-4V alloy	—	Turning	Surface roughness (R_a)
[11]	Ramesh et al., 2008	Ti-6Al-4V alloy	—	Turning	Cutting force, surface Roughness (R_a), tool flank wear
[12]	Ramesh et al., 2009	Ti-6Al-4V alloy	—	Turning	Cutting force, surface Roughness (R_a), tool flank wear
[13]	Sridharan & Malkin, 2009	—	CNT & MoS_2	Grinding	G-ratio, surface roughness, specific energy
[14]	Kwon & Drzal, 2010	—	Graphite	—	—
[15]	Nam et al., 2011	Al-6061 alloy	Diamond	Micro-drilling	Drilling torque, thrust force & quality of hole
[16]	Samuel et al., 2011	—	Graphene	—	Fluid properties
[17]	Park et al., 2011	AISI 1045 steel	Graphene	Ball milling	Tribological behavior & tool wear
[18]	Vasu & Reddy, 2011	Inconel-600 alloy	Al_2O_3	Turning	Tool wear, surface roughness (R_a), cutting temperature
[19]	Ramesh et al., 2012	Ti-6Al-4V alloy	—	Turning	Surface roughness (R_a)
[20]	Khanderkar et al., 2012	AISI 4340	Al_2O_3	Turning	Wettability, cutting force, tool wear, surface roughness (R_a), chip morphology & chip thickness
[21]	Kalita et al., 2012	EN 24 alloy steel	MoS_2	Grinding	Specific energy, friction coefficient, Grinding (G)-ratio
[22]	Nguyen et al., 2012	AISI 1045 steel	xGnP & hBN nano-platelets	Ball milling	Tribological behavior & tool wear
[23]	Amrita et al., 2013	AISI 1040 steel	Graphite	Turning	Cutting force, cutting temperature, tool wear
[24]	Paul & Varadarajan, 2013	AISI 4340 steel	Semi-Solid Lubricants	Turning	Cutting force, cutting temperature, tool wear & surface roughness (R_a), tool vibrations
[25]	Srikiran et al., 2014	AISI 1040 steel	Nano-crystalline graphite powder	Turning	Cutting forces, tool temperature & surface roughness (R_a)
[26]	Amrita et al., 2014	AISI1040 steel	Graphite	Turning	Cutting force, cutting temperature, tool wear, surface roughness (R_a), chip morphology
[27]	Sharma et al., 2015	AISI D2 steel	CNT	Turning	Cutting temperature, surface roughness (R_a)
[28]	Su et al., 2015	AISI 1045 steel	Graphite	Turning	Dynamic viscosity, surface tension, wettability, thermal conductivity, cutting forces, cutting temperature
[5]	Gupta et al., 2016	Titanium alloy	Graphite, MoS_2 & Al_2O_3	Turning	Cutting force, cutting temperature, tool wear & surface roughness (R_a)
[29]	Barzani et al., 2015	Al–Si–Cu cast alloy	Dry	Turning	Surface roughness and cutting force
[30]	Barzani et al., 2015	Al–Si–Cu–Fe die casting alloy	Dry	Turning	Prediction of average surface roughness using Fuzzy logic
[31]	Unune et al., 2016	Nimonic 80A	Dry	Abrasive-mixed electro-discharge diamond surface grinding	Prediction of material removal rate and average surface roughness using Fuzzy logic

*hBN = hexagonal Boron Nitride, xGnP = Graphene, CNT = Carbon nano-tubes, MoS_2 = Molybdenum disulfide, Al_2O_3 = Aluminum oxide

2.1 Materials and methods

2.2 Preparation of nano-fluids

In this study, the nano-fluids were prepared using a two-step method. The three different types of nano-particles, i.e., aluminum oxide (Al_2O_3), molybdenum disulfide (MoS_2) and graphite, each having an average diameter of 40 nm were used. Vegetable oil was chosen as the base oil due to its good biodegradability and low environmental impact. The concentrations of nano-particles in the vegetable based oils were 3 wt%. The concentration was then ultra-sonicated in a sonicator (40 kHz, 100W) (for 1 h) and magnetic stirrer (30 min), respectively. The process was repeated several times until all the nano-particles dispersed consistently within the vegetable based oil. The results indicated that the nano-fluid prepared was steady and no settlement of particles was found throughout the entire machining operation. The properties of the nano-fluids were measured and shown in Table 2.

2.2 Work material and cutting tool

For the experiments, titanium (grade-2) alloy having 50 mm diameter and 150 mm length was used. The chemical composition of the selected material is shown in Table 3. The cubic boron nitride inserts (CCGW 09T304-2, Positive 7°, Clearance 80°, rhombic, nose radius 0.4 mm) were used for performing the experiments.

2.3 Turning tests

A high precision CNC turning center (Sprint 16 TC equipped with a Siemens control system) having three simultaneously controlled axes (X, Y, and Z axis), was used for machining the given alloy. The NFMQL set up used in the current investigation was imported from Israel (NOGA made, mini cool system). The flow rate of 30 ml/h, air flow rate and pressure of 60 L/min and 5 bar, respectively were fixed throughout the turning experiments.

2.4 Surface roughness measurements

Surface roughness is defined as the finer irregularities of the surface texture that usually result from the inherent action of the machining process. The portable roughness tester (SJ301-MITUTOYO make) was used for measuring the three surface roughness values, i.e., average roughness (R_a), root mean square (R_q) and maximum peak to valley (R_z). The roughness tester has three measuring driving units namely the standard drive unit, the transverse tracing drive unit and the retractable drive unit. In the present study, the measurements have been taken with the standard drive unit according to the ISO 97 R standard, which includes the measuring force of 4 mN, stylus tip radius of 5 μm and tip material diamond and conical-taper angle of 90°. Moreover, one height stand is used (to hold and adjust the surface roughness tester), one surface plate and one V-block are required for the workpiece placement. The complete procedure for measuring the surface roughness is discussed here. Firstly, a stylus with the help of a moving height stand is adjusted on the machine surface of the workpiece, which is placed on the V-Block. Then, the center line of the stylus tip and workpiece has been matched. When the stylus is moved on the center "cut" lines made by the point cutting tool, the readings are displayed on the screen. After that, the workpiece is rotated three times at an angle of 120° and measures the surface roughness values. Finally, the mean of all three surface roughness values are considered. Figure 1 explains the measurement procedure of the surface roughness. In the end, the machined surface of titanium (grade-2) was characterized by scanning electron microscopy (SEM, Bruker make).

Table 2 Properties of nano-fluids.

Properties	Vegetable based oil	Al_2O_3 nano-fluid	MoS_2 nano-fluid	Graphite nano-fluid
Appearance	Bright and clear	White	Black	Grayish black
Viscosity (CP) (at 20 °C)	68.16	120.23	100.56	83.12
Thermal conductivity (W/(m·K))	0.1432	0.2085	0.2362	0.2663

Table 3 Chemical composition of Titanium (grade-2).

C	Fe	H	O	N	Ti
0.1% max	0.3%	0.015%	0.25%	0.03%	99.2%

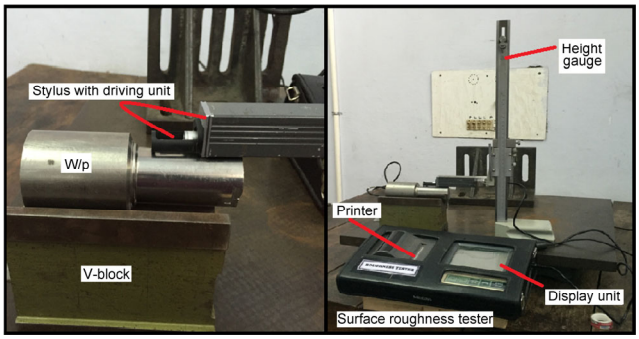

Fig. 1 Equipments used to measure the surface roughness values.

2.5 Cutting parameters and their levels

The turning tests were performed at different levels of cutting speed, feed rate, approach angle and different nano-fluids. A poor surface finish due to premature tool failure was observed at higher level of cutting speed (>300 m/min). However, no such phenomenon occurred when turning at lower cutting speed (>200 m/min). Therefore, the cutting speed range of 200–300 m/min was selected for turning of titanium (grade-2) alloy under NFMQL conditions, whereas feed rate and approach angle ranges were decided based on literature reviews and tool manufacturer's recommendations. A constant depth of cut of 1 mm was used for the experiments. The complete experimental procedure is displayed in Fig. 2.

2.6 Design of experiment

The purposed methodology is divided into the following stages. Firstly, the experiments were designed and planned using the Box-Behnkens RSM technique. It is a group of numerical and measurable strategies

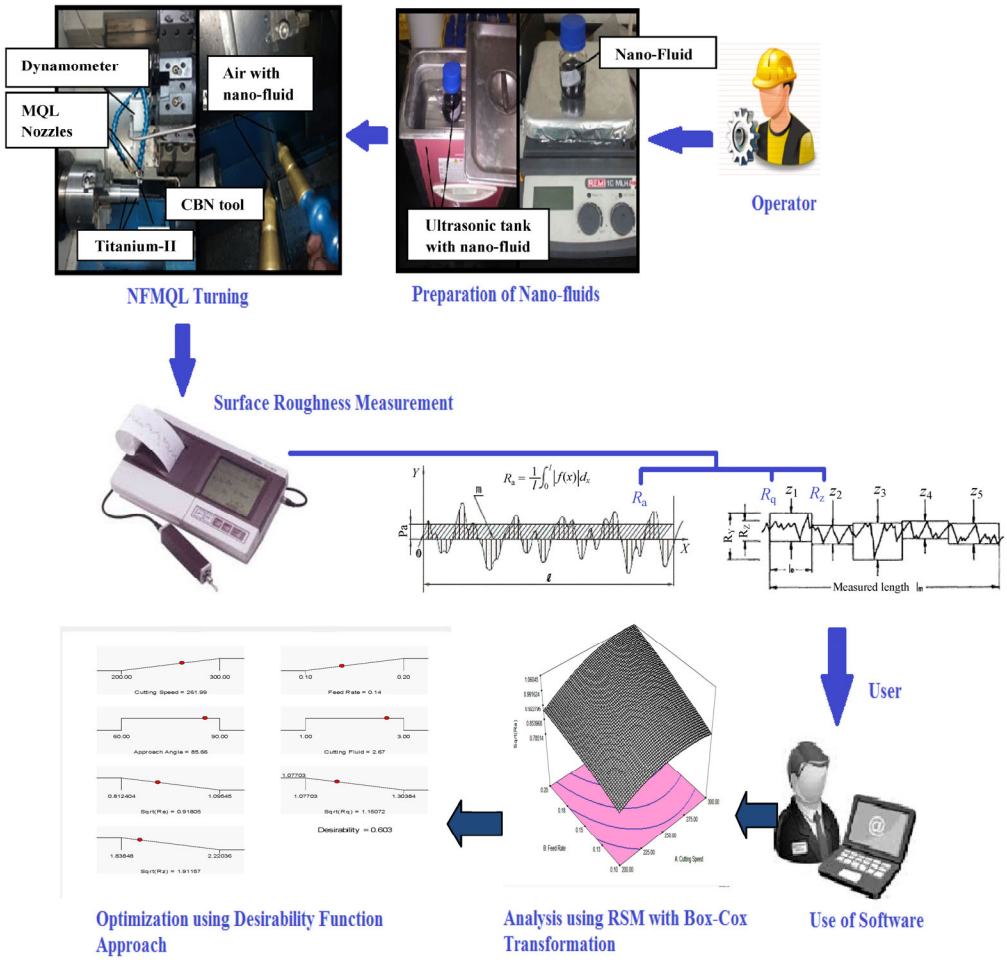

Fig. 2 Experimental procedure used to determine surface roughness values.

that are helpful for displaying and examining issues in which a reaction of interest is impacted by a few variables and the goal is to improve this output [32–34]. The experimental conditions and results of the given responses are tabulated in Table 4. In the second stage, the predictive models are established with the help of regression equations and the Box-Cox transformation. Generally, the Box–Cox transformation gives a group of changes to standardize the information, which is not typically conveyed by distinguishing a fitting example (lambda, λ). The lambda demonstrates the ability to which all information ought to be raised. The Box-Cox transformation initially imagined this change as a panacea for and at the same time revising typicality, linearity and homogeneity. In the third stage, the multi-response optimization is performed by using the desirability function approach. The flowchart of the RSM technique is shown in Fig. 3.

Table 4 Machining parameters with the experimental design and their results.

Sr. No.	V_c (m/min)	f (mm/rev)	ϕ (°)	Nano-fluids*	R_a (μm)	R_q (μm)	R_z (μm)
1	300	0.15	75	3	0.90	1.48	4.15
2	250	0.15	75	2	0.92	1.42	3.51
3	250	0.15	75	2	0.91	1.41	3.50
4	250	0.1	90	2	0.74	1.18	3.46
5	250	0.1	75	3	0.68	1.24	3.63
6	250	0.2	60	2	1.10	1.62	4.73
7	250	0.15	75	2	0.92	1.42	352
8	250	0.15	90	1	0.88	1.38	4.03
9	300	0.15	90	2	0.98	1.40	4.02
10	200	0.15	90	2	0.72	1.22	3.74
11	250	0.15	90	3	0.80	1.30	3.98
12	250	0.2	75	1	1.12	1.54	4.38
13	250	0.15	75	2	0.92	1.42	3.51
14	200	0.15	75	1	0.79	1.27	3.42
15	250	0.2	90	2	1.04	1.60	4.83
16	300	0.15	75	1	1.08	1.46	4.59
17	300	0.2	75	2	1.02	1.70	4.93
18	200	0.15	75	3	0.71	1.21	3.38
19	250	0.15	60	1	1.08	1.58	4.38
20	250	0.15	75	2	0.91	1.41	3.52
21	300	0.15	60	2	0.96	1.58	4.48
22	250	0.2	75	3	1.2	1.52	4.68
23	200	0.15	60	2	0.77	1.27	3.86
24	250	0.1	60	2	0.82	1.32	4.12
25	300	0.1	75	2	0.70	1.28	4.08
26	200	0.2	75	2	0.78	1.28	3.67
27	200	0.1	75	2	0.66	1.16	3.40
28	250	0.1	75	1	0.78	1.20	4.73
29	250	0.15	60	3	1.02	1.52	3.81

*Cutting fluid: 1—Signifies Al_2O_3 based nano-fluid, 2—signifies MoS_2 based nano-fluid, and 3—signifies graphite based nano-fluid.

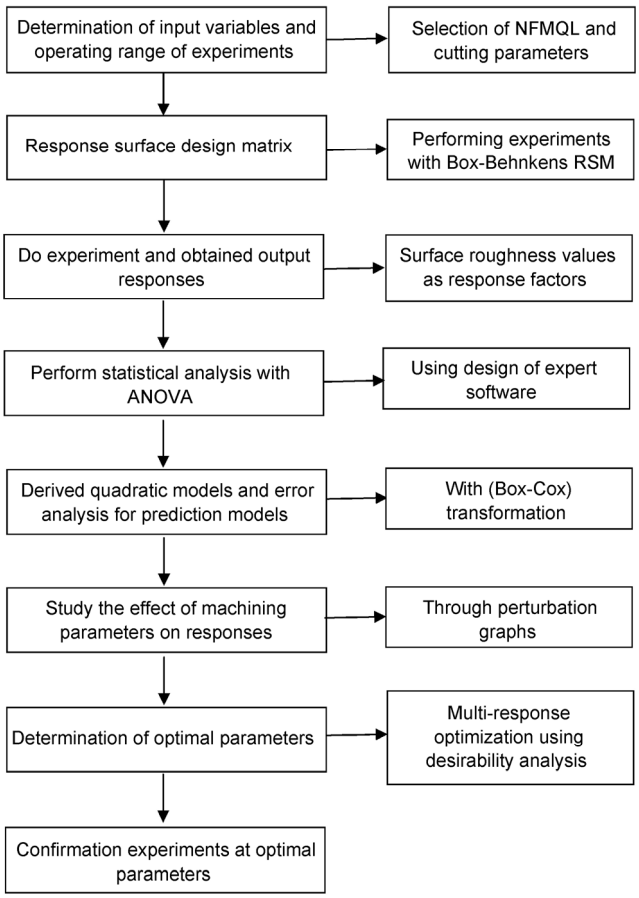

Fig. 3 Flow chart of the response surface methodology (RSM) technique.

3 Results and discussion

The experimental results obtained from Table 4 were used to establish the prediction models for R_a, R_q and R_z through RSM with the Box-Cox transformation. The adequacy of the established models was affirmed with the help of ANOVA. Then, the square root change on the reaction is required to make the residuals regularly disseminated. Finally, the error analysis of the predictive models and effect of the machining parameters on surface roughness were investigated and discussed.

3.1 Development of the prediction model with transformation for R_a, R_q and R_z

The best-fit equations to relate the responses (R_a, R_q and R_z) to the cutting parameters (V_c, f, φ and C.F.) are achieved by adapting general measurable techniques of regression analysis with the benefit of design expert software. In the case of the R_a and R_q (Table 5 and Table 6, respectively) a linear model is selected, and the cutting speed (V_c), the feed rate (f) as well as the nano-fluid (C.F.) are the significant model terms. Whereas, for R_z (Table 7) the quadratic model is suggested and the main effect of cutting speed, feed rate and nano-fluid, second-order effect of feed rate, approach angle (φ) and nano-fluid, interaction effect of feed rate and nano-fluid are the noteworthy terms. The Prob > F" from ANOVA for all demonstrations are less than 0.0500; hereafter, the models are thought to be adequate. The correlation coefficient (R^2 close to unity) was persistent to depict the adequacy of a fitted regression models and it was found that for all models R^2 was close to solidarity. Moreover, there is reasonable agreement between the "Pred R-Squared" and "Adj R-Squared" values, which confirms the adequacy of the model. The adequate precision ratio of all established models (ratio>4 is desirable) provides a satisfactory indication to utilize the proposed model. The final regressions Eqs. (1)–(3) with the square root transformation for R_a, R_q and R_z are represented as:

$$\sqrt{R_a} = 0.59012 + 1.08538\text{E-}003 \times V_c + 1.65475 \times f - 1.72109\text{E-}003 \times \varphi - 0.019258 \times \text{C.F.} \quad (1)$$

$$\sqrt{R_q} = 0.86963 + 1.05573\text{E-}003 \times V_c + 1.32362 \times f - 1.89800\text{E-}003 \times \varphi - 5.61066\text{E-}003 \times \text{C.F.} \quad (2)$$

$$\sqrt{R_z} = 5.07360 + 1.99235\text{E-}003 \times V_c - 15.11368 \times f - 0.053138 \times \varphi - 0.56240 \times \text{C.F.} + 44.21514 \times f^2 + 3.41977\text{E-}004 \times \varphi^2 + 0.067071 \times \text{C.F.}^2 + 1.70043 \times f \times \text{C.F.} \quad (3)$$

Furthermore, in order to confirm the adequacy or efficacy of the develped model, diagnostic plots were used. They guarantee that the measurable theory fits the systematic information accodingly. Figure 4 uncovers that, in the case of R_a the residuals for all demonstrations fall on a straight line, which signifies that the errors were normally distributed. The simillar trend is observed for the remaining responses, i.e., for R_q and R_z, which confirms the adequacy of the developed models. Simillarly, Fig. 5 shows a Box–Cox plot for power transformation with respect to R_a. For all the models, the blue line indicates the current value of lambda for residuals as 0.5, which lie outside

Table 5 ANOVA for R_a with transformation.

Source	Sum of squares	DF	Mean square	*F* value	Prob > *F*	Remarks
Model	0.129937	4	0.032484	18.48896	< 0.0001	Significant
V_c	0.035342	1	0.035342	20.11545	0.0002	
f	0.082146	1	0.082146	46.75517	< 0.0001	
φ	0.004451	1	0.004451	2.533099	0.1246	
C.F.	0.007998	1	0.007998	4.552105	0.0433	
Residual	0.042167	24	0.001757			
Lack of fit	0.042134	20	0.002107	257.0153	< 0.0001	Significant
Pure error	3.28E-05	4	8.2E-06			
Cor total	0.172103	28				
Std. Dev.	0.041916		R-Squared	0.754992		
Mean	0.942079		Adj R-Squared	0.714157		
C.V.	4.449302		Pred R-Squared	0.619395		
PRESS	0.065503		Adeq Precision	15.74371		

Table 6 ANOVA for R_q with transformation.

Source	Sum of squares	DF	Mean square	*F* value	Prob > *F*	Remarks
Model	0.096101	4	0.024025	38.94489	< 0.0001	Significant
V_c	0.033437	1	0.033437	54.20177	< 0.0001	
f	0.052559	1	0.052559	85.19868	< 0.0001	
φ	0.000378	1	0.000378	0.612342	0.4416	
C.F.	0.009727	1	0.009727	15.76676	0.0006	
Residual	0.014806	24	0.000617			
Lack of fit	0.014784	20	0.000739	139.466	0.0001	Significant
Pure error	2.12E-05	4	5.3E-06			
Cor total	0.110906	28				
Std. Dev.	0.024837		R-Squared	0.866503		
Mean	1.178531		Adj R-Squared	0.844254		
C.V.	2.107497		Pred R-Squared	0.793814		
PRESS	0.022867		Adeq Precision	23.07093		

the 95% confidence limit. But the best recommended value of lambda is approximately −0.42 for R_a, −0.61 for R_q and −1.06 for R_z as shown by the green line. The optimum Box-Cox transformation was calculated by finding the value of lambda that maximizes the negative log likelihood. Moreover, from ANOVA it was found that the feed rate is the most effective parameter followed by cutting speed, different nano-fluids and approach angle on R_a and R_q values under NFMQL conditions; whereas cutting speed is more effective in the case of R_z.

3.2 Error analysis for prediction models

In order to verify the predictiveness of the established models using the Box-Cox transormation, an error analyis based on statistical methods of percentage mean absolute error (%MAE) and percentage mean square error (%MSE) was performed. These values

Table 7 ANOVA for reduced quadratic model for R_z with transformation.

Source	Sum of squares	DF	Mean square	F value	Prob > F	Remarks
Model	0.366231	8	0.045779	15.54117	< 0.0001	Significant
V_c	0.119083	1	0.119083	40.42686	< 0.0001	
f	0.072236	1	0.072236	24.52277	< 0.0001	
φ	0.009156	1	0.009156	3.108434	0.0932	
C.F.	0.018303	1	0.018303	6.213477	0.0216	
f^2	0.082198	1	0.082198	27.90486	< 0.0001	
φ^2	0.039829	1	0.039829	13.52122	0.0015	
C.F.^{2}	0.030263	1	0.030263	10.27386	0.0044	
f*C.F.	0.028915	1	0.028915	9.816054	0.0052	
Residual	0.058913	20	0.002946			
Lack of fit	0.058893	16	0.003681	738.4153	< 0.0001	Significant
Pure error	1.99E-05	4	4.98E-06			
Cor total	0.425144	28				
Std. Dev.	0.054274		R-Squared	0.861428		
Mean	1.996677		Adj R-Squared	0.805999		
C.V.	2.718209		Pred R-Squared	0.6685		
PRESS	0.140935		Adeq Precision	12.32878		

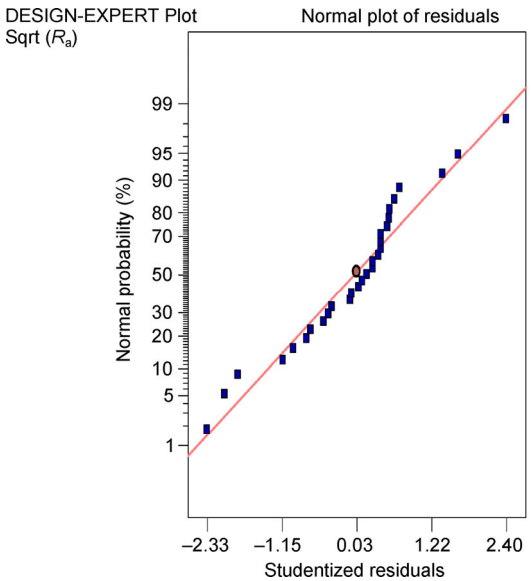

Fig. 4 Normal probability plot for R_a.

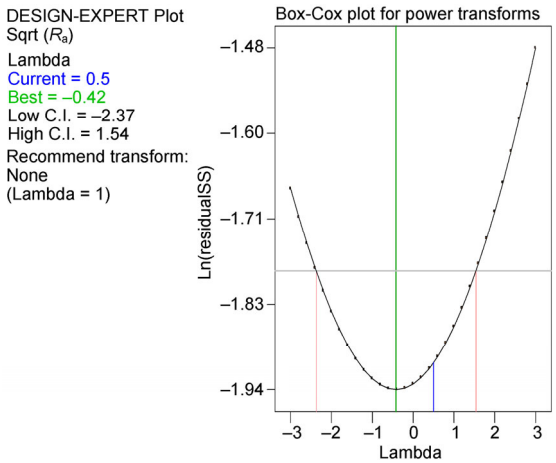

Fig. 5 Box-Cox power transformation plots for R_a.

were determined using Eqs. (4)–(5), respectively:

$$\%\ \mathrm{MAE} = \left(\frac{1}{n}\sum_i \left|\frac{e_i - p_i}{e_i}\right|\right)\times 100 \quad (4)$$

$$\%\ \mathrm{MSE} = \left(\frac{1}{n}\sum_i |e_i - p_i|^2\right)\times 100 \quad (5)$$

where e is the experimental value, p is the predicted value and n is the number of iterations for experimentation. From the error analysis, it was found that the value of maximum percentage absolute error reduces from 48.56 to 8.79 for R_a, 36.78 to 111.42 for R_q, and 56.63 to 9.69 for R_z using a Box–Cox transformation. Furthermore, the maximum percentage square error reduces from 8.23 to 0.421 for R_a, 7.96 to 0.134 for R_q, and 16.33 to 1.914 for R_z. This indicates the better prediction ability of the developed models using the Box–Cox transformation.

In the end, the adequacy of the developed model is

validated and checked by comparing the predicted and experimental surface roughness values. Figure 6 represents the comparative assesment of the predicted and experimental values for R_a. As shown in Fig. 6, it was found that the predicted values for R_a are very closer to the experimental values and the errors are also found to be much less, which confirms good efficacy of the developed model. The same trend is found for the remaining responses and good agreement is observed between these values. Hence, an application of RSM with the Box-Cox transformation was found to be an effective method for identification and development of models within the seletced ranges of cutting parameters.

3.3 Effect of machining parameters on surface roughness values

The influence of all cuttting parameters after the Box-Cox transformation on average surface roughness was performed with the help of perturbation analysis, as shown in Figs. 7(a)–7(c).

Effect of cutting speed on R_a, R_q and R_z: Cutting speed greatly influenced all surface roughness values, i.e., R_a, R_q, and R_z. So the three values of cutting speed (200, 250, 300 m/min) have been considered for the current investigation. The characterization of machined samples is performed at the preferred machining parameters. It was found that, in the case of NFMQL turning during sticky material like titanium (grade-2), the values of surface roughness moderately increase with the change in cutting speed from 200 m/min to 300 m/mn. This might occur because, at higher values of cutting speeds, the major portion of the chips will move from the tool cutting edge and generate high friction, which results in higher values of surface roughness. Also, the high cutting speed creates the built up edge at the tool, thus lowering the surface finish.

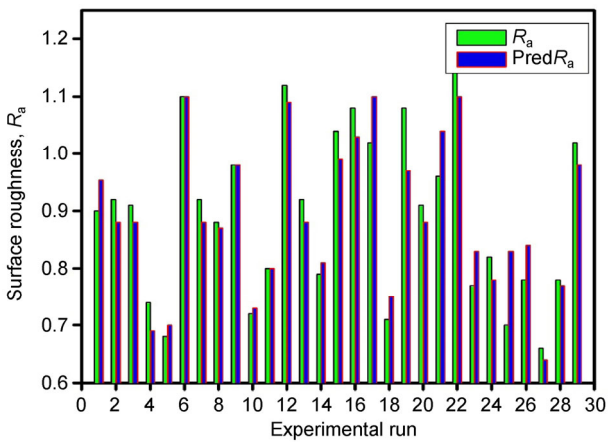

Fig. 6 Surface roughness as a function of experimental run using predicted and experimental R_a.

Effect of feed rate on R_a, R_q, and R_z: Due to the high ductility of titanium and its alloys, the built up edge are formed on the tool rake face. At the point when the impact of the built-up edge is viewed as unimportant, the cutting tool profile, i.e., curved or pointed gets embossed on the workpiece and the surface roughness starting here relies on upon the feed rate. Furthermore, it is well known fundamental of metal cutting that, the pitch of the surface to be machined is greatly affected by the feed rate ($R_a = \frac{f^2}{32r}$). This explains why the surface roughness is sharply incremented with the increase in feed rate from 0.10 mm/rev to 0.20 mm/rev. Also, it has been found that the tool moves very qucikly at higher cutting speed and feed rates, resulting in deteriorated surface quality, machine chattering and vibrations. Hence, the leads to higher surface roughness values. Gupta et al. also discovered the similar results [35].

Effect of approach angle on R_a, R_q and R_z: The main cutting edge moves towards the workpiece with an approaching angle. For large approach angles, the contact surface is distributed over a shorter section of the cutting edge whereas with small approach angles, it is spread over a greater length. The thickness of the cutting chip also depends on the approach angle. The approach angle plays an important role in the tool's life, therefore it is imperative to evaluate the effect of approach angle on other parameters such as surface roughness by keeping the speed and feed constant. It is for this reason that with the increased approach angles, the contact length of the cutting tool tip with respect to the work material is less, which further decreases the friction between the tool and work piece, which leads to low vibration in the machining and increases the surface finishing.

Effect of different nano-fluids on R_a, R_q and R_z: The change in nano-fluid also shows surprising results on the surface roughness values. It has been found that, the values of surface roughness decrease with the change in nano-fluid from aluminum-oxide based nano-fluid to graphite based nano-fluid. Because the

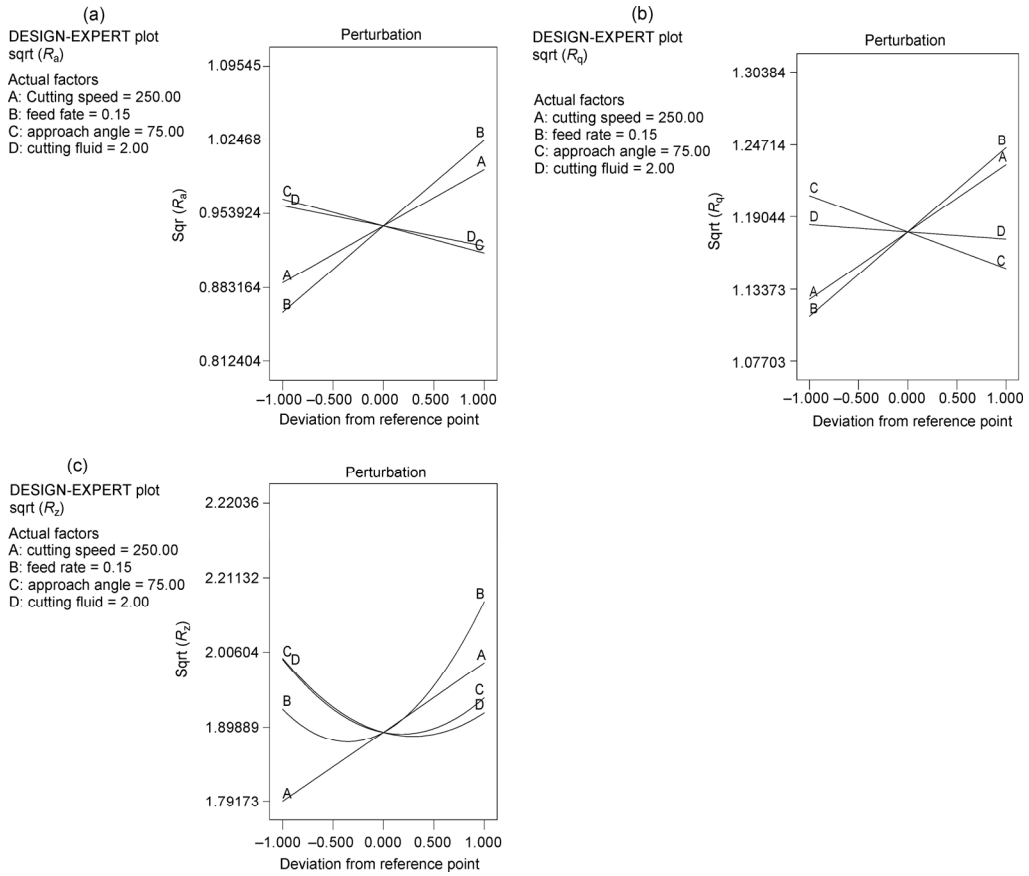

Fig. 7 Perturbation graphs for: (a) R_a, (b) R_q, and (c) R_z.

viscosity of graphite is lower compared to the other two fluids, which results in the proper settlement of the nano-fluids between the workpiece and the tool, hence, this provides the cushioning effect which may induce low machine chattering and vibrations and increase the surface finishing of the titanium (grade-2) alloy. Moreover, the decrease in surface roughness values with graphite based nano-fluid is also associated with its thermal conductivity. The higher thermal conductivity of graphite based nano-fluids helps to dissipate the heat from the primary cutting zone, which leads to less tool wear. Less tool wear helps in accomplishing better surface quality by diminishing the redeposition of materials on the machined surface. The same trend was examined by Sharma et al. [27]. Figure 8 uncovers the reduced redeposition on the machined surface while utilizing graphite-based nano-fluids. Figure 9 depicts that feed marks are clealry

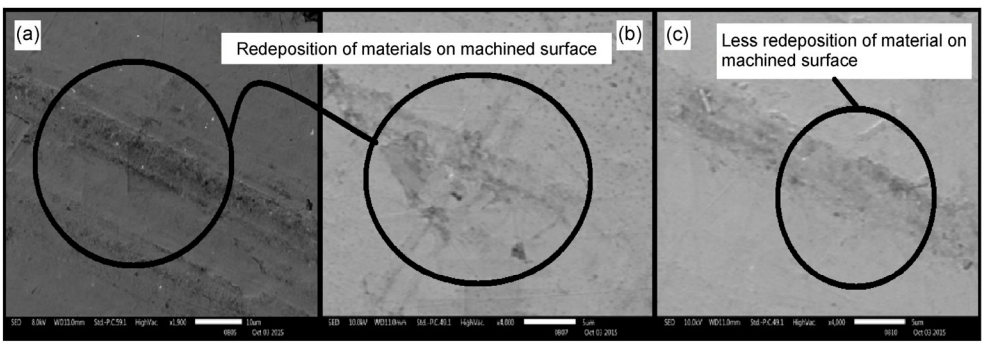

Fig. 8 Machined surface at cutting speed = 250 m/min, feed rate = 0.2 mm/rev and approach angle = 75°: (a) Al_2O_3 based nano-fluid, (b) MoS_2 based nano-fluid, and (c) graphite based nano-fluid.

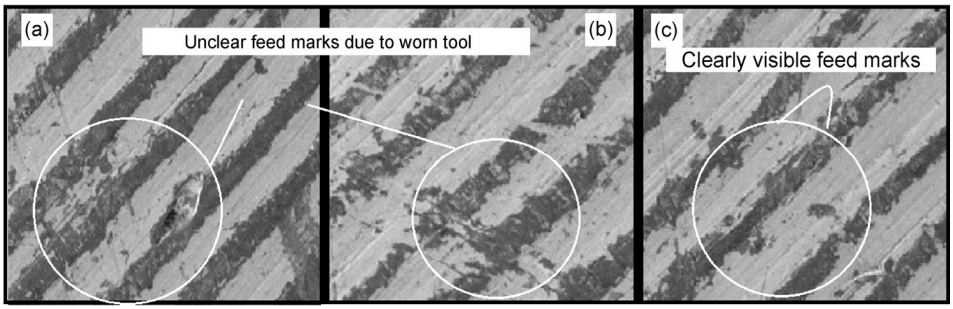

Fig. 9 Machined surface at cutting speed = 250 m/min, feed rate = 0.2 mm/rev and approach angle = 75°: (a) Al_2O_3 based nano-fluid, (b) MoS_2 based nano-fluid, and (c) graphite based nano-fluid.

visible and clean surface are obtained without any plastic deformation under graphite based nano-fluids as compared to others.

4 Desirability based multi response optimization

The desirability based multi response optimization is performed to obtain minimal surface roughness values. In this study, the ranges of input parameters viz. cutting speed and feed rate are selected to be maximum, whereas the approach angle and nano-fluids are selected within ranges shown in Table 8. An arrangement of three ideal solutions are determined for the particular design space constraints for surface roughness values by using the design expert statistical software. The arrangement of conditions having the most desirability value is chosen as ideal conditions for the given outputs. Once the ideal level of the procedure parameters is chosen, the last stride is to predict and confirm the enhancement of the performance characteristics utilizing the ideal level of the machining parameters [35]. The ramp function graph for the desired objectives was selected as shown in Fig. 10. The point on every ramp shows the parameter setting or output prediction for that output characteristic. The height of every point demonstrates the level of desirability. Furthermore, the contour plots for overall desirability has been plotted to show the sensitivity of the results as shown in Fig. 11. The near optimal area was positioned close to the the left hand base area of the plot, which had a general desirability value more prominent than 0.6 that slowly decreased as we moved right and upwards. Sensitivities are acquired utilizing the shape of the contour lines in Fig. 11. The optimal values are tabulated in Table 9.

Table 8 Range of input parameters and responses for desirability optimization.

Parameter	Goal	Lower limit	Upper limit	Lower weight	Upper weight	Importance
Cutting speed	maximize	200	300	1	1	3
Feed rate	maximize	0.1	0.2	1	1	3
Approach angle	is in range	60	90	1	1	3
Nano-fluid	is in range	1	3	1	1	3
Sqrt (R_a)	minimize	0.812404	1.095445	1	1	3
Sqrt (R_q)	minimize	1.077033	1.30384	1	1	3
Sqrt (R_z)	minimize	1.83848	2.22036	1	1	3

Table 9 Optimization results.

Sr. No.	Cutting speed	Feed rate	Approach angle	Nano-fluid	Sqrt (R_a)	Sqrt (R_q)	Sqrt (R_z)	Desirability	
1	253.55	0.14	87.04	3	0.899	1.146	1.913	0.615721	Selected
2	245.17	0.13	87.28	2	0.883	1.124	1.895	0.502346	
3	273.89	0.14	72.25	2	0.961	1.200	1.937	0.501354	

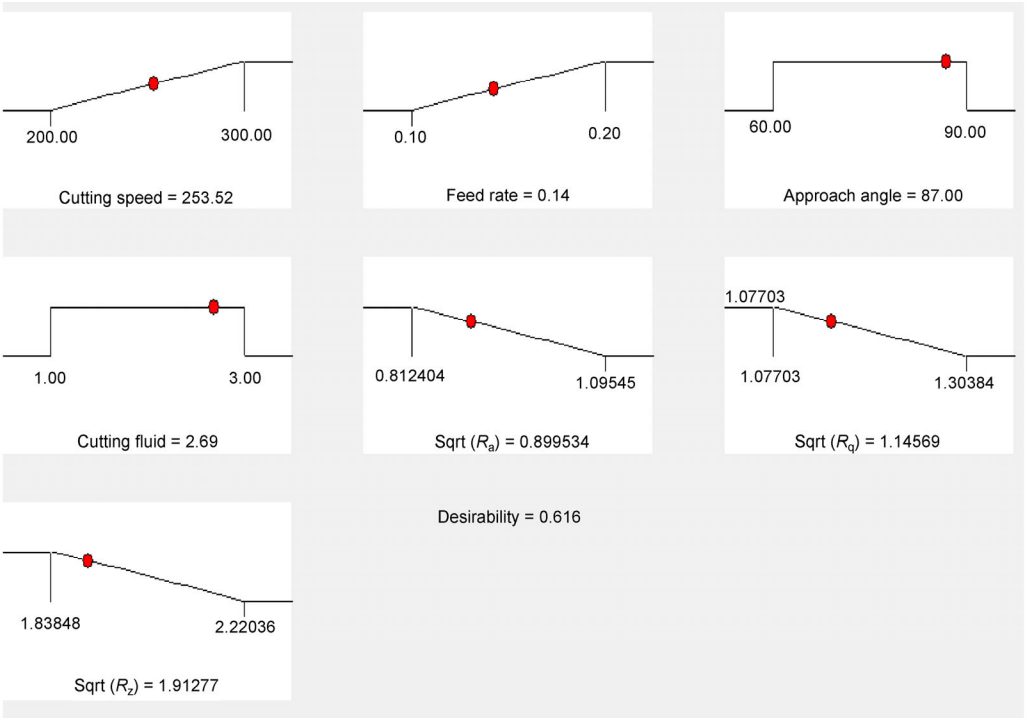

Fig. 10 Ramp function graphs of desirability optimizations.

Then, the confirmation experiments have been performed to validate the established model as presented in Table 10. The predicted and experimental values are near to each other, which demonstrates the importance of the established models.

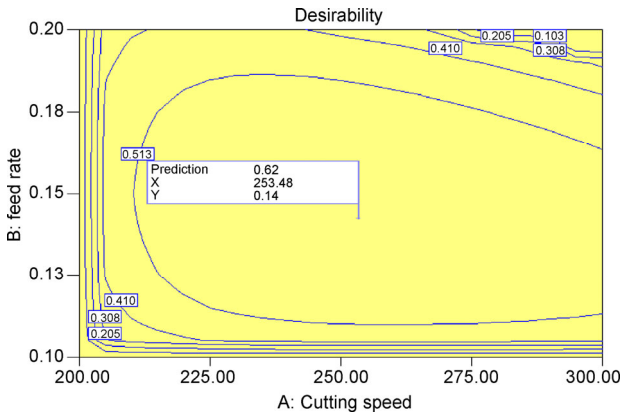

Fig. 11 Contour plots for result of overall desirability function (cutting speed vs. feed rate).

5 Conclusion

In the present work, nano-fluid based MQL environments are developed to meet the the demands for environmentally friendly machining processes. The effect of the machining variables (cutting speed, feed rate and approach angle) and different nano-fluids on three surface roughness values in turning of titanium-II under NFMQL conditions has been investigated. Then, the surface roughness prediction model using RSM with the Box-Cox transformation has been established. The following conclusions are drawn from the analysis of the results within the selected range of parameters:

1. The outcomes demonstrate that, feed rate is the most effective parameter followed by cutting speed, different nano-fluids and approach angle on R_a and

Table 10 Confirmation test for the optimization value.

Parameters	Initial result at optimum value	Experimental result at optimum value
Cutting speed	253.55	253.55
Feed rate	0.14	0.14
Approach angle	87	87
Nano-fluid	3	3
Sqrt (R_a)	0.899	0.874
Sqrt (R_q)	1.146	1.1123
Sqrt (R_z)	1.913	1.803

R_q under NFMQL conditions, whereas cutting speed is more effective in the case of R_z.

2. It has been observed that as in the case of NFMQL turning during sticky materials like titanium (grade-2), the values of surface roughness moderately increase due to the rise in cutting speed, whereas it sharply increases due to the rise in feed rate. This might occur because, at higher values of cutting speeds, the major portion of the chips will move from the tool's cutting edge and generates high friction, which results in higher values of surface roughness.

3. However, with increasing in approach angles the contact length of the cutting tool tip with respect to the work material is less, which further decreases the friction between the tool and the work piece, which leads to low vibration in the machining and an increase in the surface finishing.

4. The change in nano-fluid also shows surprising results on the surface roughness values. It has been found that, the values of surface roughness decrease with the change in nano-fluid from aluminum-oxide based nano-fluid to graphite based nano-fluid. Because the viscosity of graphite is lower compared to the other two fluids, this results in proper settlement of the nano-fluids between the workpiece and the tool, hence, which provides the cushioning effect which may induce low machine chattering and vibrations and increase the surface finishing of the titanium (grade-2) alloy.

5. The RSM with the Box-Cox transformation was found to be an effective method for identification and development of significant relationships between the cutting parameters and the given responses.

6. The contour effect plots for overall desirability function revealed the desirability range when responses are given equal weighting. It shows that the cutting speed of 253 m/min, the feed rate of 0.14 mm/rev, the approach angle of 87° and the graphite based nano-fluids are desirable for obtaining the optimal conditions.

The results clearly showed that this optimisation method was effective and incredibly diminished the machining cost. This model can be efficiently applied to find the suitable cutting conditions, in order to achieve the preferred surface roughness value. The future empirical work will look into the effect of different parameters such nose radius, tool materials, work materials, etc. on the surface roughness values under NFMQL conditions.

Acknowledgement

The authors are extremely grateful to Dr. Vishal S. Sharma, NIT Jalandhar for providing the research facilities. Authors also acknowledge the MHRD, Govt. of India and Central Workshop NIT Hamirpur (H.P.) for the financial support.

References

[1] Routara B C, Bandyopadhyay A, Sahoo P. Roughness modeling and optimization in CNC end milling using response surface method: effect of work piece material variation. *Int J Adv Manuf Technol* **40**: 1166–1180 (2008)

[2] Davim J P, Gaitonde V N, Karnik S R. Investigations into the effect of cutting conditions on surface roughness in turning of free machining steel by ANN models. *J Mater Process Technol* **205**: 16–23 (2007)

[3] Bhardwaj B, Kumar R, Singh P K. Surface roughness (Ra) prediction model for turning of AISI 1019 steel using response surface methodology and Box-Cox transformation. *Proc IMechE, Part B: J Eng Manuf* **228(2)**: 223–232 (2013)

[4] Sharma V S, Dogra M, Suri N M. Cooling techniques for improved productivity in turning. *Int J Mach Tool Manu* **49(6)**: 435–453 (2009)

[5] Gupta M K, Sood P K, Sharma V S. Optimization of machining parameters and cutting fluids during nano-fluid based minimum quantity lubrication turning of titanium alloy by using evolutionary techniques. *J Cleaner Production* **135:** 1276–1288 (2016)

[6] Dureja JS, Singh R, Singh T, Singh P, Dogra M, Bhatti M S.. Performance evaluation of coated carbide tool in machining of stainless steel (AISI 202) under minimum quantity

lubrication (MQL). *Int J Precis Eng Manuf* **2**: 123–129 (2015)

[7] Gupta M K, Sood P K, Sharma V S. Machining parameters optimization of titanium alloy using response surface methodology and particle swarm optimization under minimum quantity lubrication environment. *Mater Manuf Process* **31:** 1671–1682 (2016)

[8] Sharma VS, Singh G, Sorby K. A review on minimum quantity lubrication for machining processes. *Mater Manuf Process* **30**(8): 935–953 (2015)

[9] Shen B, Malshe A P, Kalita P, Shih A J. Performance of novel MOS_2 nano-particles based grinding fluids in minimum quantity lubrication grinding. *Trans NAMRI/SME* **36**: 357–364 (2008)

[10] Ramesh S, Karunamoorthy L, Palanikumar K. Surface roughness analysis in machining of titanium alloy. *Mater Manuf Process* **23**(2): 174–181 (2008)

[11] Ramesh S, Karunamoorthy L, Palanikumar K. Fuzzy Modeling and analysis of machining parameters in machining titanium alloy. *Mater Manuf Process* **23**(4): 439–447 (2008)

[12] Ramesh S, Karunamoorthy L, Senthilkumar V S, Palanikumar K. Experimental study on machining of titanium alloy (Ti64) by CVD and PVD coated carbide inserts. *Int J Manuf Technol Manag* **17**(4): 373–385 (2009)

[13] Sridharan U, Malkin S. Effect of minimum quantity lubrication (MQL) with nano-fluid on grinding behavior and thermal distortion. *Trans NAMRI/SME* **37:** 629–636 (2009)

[14] Kwon P, Drzal L T. Nanoparticle graphite-based minimum quantity lubrication method and composition. U.S. Patent **649**: 12–655, 2010.

[15] Nam J S, Lee P H, Lee S W. Experimental characterization of micro-drilling process using nano-fluid minimum quantity lubrication. *Int J Mach Tool Manuf* **51**(7–8): 649–652 (2011)

[16] Samuel J, Rafiee J, Dhiman P, Yu Z Z, Koratkar N. Graphene colloidal suspensions as high performance semi-synthetic metal-working fluids. *J Phys Chem C* **115**(8): 3410–3415 (2011)

[17] Park K H, Ewald B, Kwon P Y. Effect of nano-enhanced lubricant in minimum quantity lubrication balling milling. *J Tribol* **133**: 031803 (2011)

[18] Vasu V, Reddy P K G. Effect of minimum quantity lubrication with Al_2O_3 nanoparticles on surface roughness, tool wear and temperature dissipation in machining Inconel 600 alloy. *Proc Inst Mech Eng Part N J Nanoeng and Nanosyst* **225**: 3–16 (2011)

[19] Ramesh S, Karunamoorthy L, Palanikumar K. Measurement and analysis of surface roughness in turning of aerospace titanium alloy (gr5). *Measurement* **45:** 1266-1276 (2012)

[20] Khandekar S, Sankar M R, Agnihotri V, Ramkumar J. Nano-cutting fluid for enhancement of metal cutting performance. *Mater Manuf Process* **27**(9): 963–967 (2012)

[21] Kalita P, Malshe A P, Arun Kumar S, Yoganath V G, Gurumurthy T. Study of specific energy and friction coefficient in minimum quantity lubrication grinding using oil-based nanolubricants. *J Mater Process Technol* **14**: 160–166 (2012)

[22] Nguyen T K, Do I, Kwon P. A tribological study of vegetable oil enhanced by nano-platelets and implication in MQL machining. *Int J Prec Eng Manuf* **13(7)**: 1077–1083 (2012)

[23] Amrita M, Srikant R, Sitaramaraju A, Prasad M, Krishna P V. Experimental investigations on influence of mist cooling using nanofluids on machining parameters in turning AISI 1040 steel. *Proc Inst Mech Eng Part J J Eng Tribol* **227:** 1334–1346 (2013)

[24] Paul P S, Varadarajan A S. Performance evaluation of hard turning of AISI 4340 steel with minimal fluid application in the presence of semi-solid lubricants. *Proc Inst Mech Eng Part J J Eng Tribol* **227**: 738–748 (2013)

[25] Srikiran S, Ramji K, Satyanarayana B, Ramana S. Investigation on turning of AISI 1040 steel with the application of nano-crystalline graphite powder as lubricant. *Proc Inst Mech Eng Part C J Mech Eng Sci* **228**: 1570–1580 (2014)

[26] Amrita M, Srikant R R, Sitaramaraju A V. Performance evaluation of nanographite-based cutting fluid in machining process. *Mater Manuf Process* **29**: 600–605 (2014)

[27] Sharma P, Sidhu B S, Sharma J. Investigation of effects of nanofluids on turning of AISI D2 steel using minimum quantity lubrication. *J Cleaner Production* **108**: 72–79 (2015)

[28] Su Y, Gong L, Li B, Liu Z, Chen D. Performance evaluation of nanofluid MQL with vegetable-based oil and ester oil as base fluids in turning. *Int J Adv Manuf Technol* **83**(9): 2083–2089 (2015)

[29] Barzani M M, Sarhan A A D, Farahany S, Ramesh S, Maher I. Investigating the machinability of Al–Si–Cu cast alloy containing bismuth and antimony using coated carbide insert. *Measurement* **62**: 170–178 (2015)

[30] Barzani M M, Zalnezhad E, Sarhan A A D, Farahany S, Ramesh S. Fuzzy logic based model for predicting surface roughness of machined Al–Si–Cu–Fe die casting alloy using different additives-turning. *Measurement* **61**: 150–161 (2015)

[31] Unune DR, Barzani MM, Mohite SS, Mali HS. Fuzzy logic-based model for predicting material removal rate and average surface roughness of machined Nimonic 80A using abrasive-mixed electro-discharge diamond surface grinding. *Neural Computing and Applications,* in press, DOI 10.1007/s00521-016-2581-4 (2016)

[32] Oudjene M, Ben-Ayed L, Delamézière A, Batoz J L. Shape optimization of clinching tools using the response surface methodology with Moving Least-Square approximation. *J Mater Process Technol* **209**: 289–296 (2009)

[33] Hewidy M S, El-Taweel T A, El-Safty M F. Modelling the machining parameters of wire electrical discharge machining of Inconel 601 using RSM. *J Mater Process Technol* **169**: 328–336 (2005)

[34] Montgomery D C. *Design and Analysis of Experiments*. New York: Wiley, 2001.

[35] Gupta M K, Sood P K, Sharma V S. Investigations on surface roughness measurement in minimum quantity lubrication turning of titanium alloys using response surface methodology and Box–Cox transformation. *J Manuf Sci Product* **16:** 75–88 (2016)

Munish Kumar GUPTA. He received his bachelor degree in mechanical engineering in 2008 from I. K. Guzral PTU, Jalandhar. After then, he was M. Tech. student at the same university. He is recently a Ph.D. research scholar in Department of Mechanical Engineering at NIT, Hamirpur. His areas of interest include machining, casting and rapid prototyping.